molecules

MDPI

Article

Unravelling the Photoprotection Properties of Garden Cress Sprout Extract

Temitope T. Abiola [1], Nazia Auckloo [1,2], Jack M. Woolley [1], Christophe Corre [1,2], Stéphane Poigny [3] and Vasilios G. Stavros [1,*]

[1] Department of Chemistry, University of Warwick, Coventry, CV4 7AL, UK; temitope.abiola@warwick.ac.uk (T.T.A.); Nazia.Auckloo@warwick.ac.uk (N.A.) jack.woolley@warwick.ac.uk (J.M.W.); C.Corre@warwick.ac.uk (C.C.)

[2] Warwick Integrative Synthetic Biology Centre and School of Life Sciences, University of Warwick, Coventry, CV4 7AL, UK

[3] Mibelle Group Biochemistry, Mibelle AG, Bolimattstrasse 1, CH-5033 Buchs, Switzerland; stephane.poigny@mibellegroup.com (S.P.)

* Correspondence: v.stavros@warwick.ac.uk (V.G.S.)

Abstract: Plants, like humans, require photoprotection against the potentially damaging effects of overexposure to ultraviolet (UV) radiation. Previously, sinapoyl malate (SM) has been identified as the photoprotective agent in thale cress. Here, we seek to identify the photoprotective agent in a similar plant, garden cress, currently used in the skincare product Detoxophane nc. To achieve this, we explore the photodynamics of both the garden cress sprout extract and Detoxophane nc with femtosecond transient electronic absorption spectroscopy. With the assistance of liquid chromatography-mass spectrometry, we determine that the main UV-absorbing compound in garden cress sprout extract is SM. Importantly, our studies reveal that the photoprotection properties of the SM in the garden cress sprout extract present in Detoxophane nc are not compromised by the formulation environment. The result suggests that Detoxophane nc containing the garden cress sprout extract may offer additional photoprotection to the end user in the form of a UV-filter booster.

Keywords: Sunscreen; UV-filter; photoprotection; nature-inspired; photodynamics; photophysics; sinapoyl malate; plant sunscreen; photochemistry; ultrafast spectroscopy

Citation: Lastname, F.; Lastname, F.; Lastname, F. Title. *Molecules* **2021**, *26*, x. https://doi.org/10.3390/xxxxx

Academic Editor: Firstname Lastname

Received: date
Accepted: date
Published: date

1. Introduction

The need for adequate protection of human skin against high doses of ultraviolet (UV) radiation exposure from the Sun has continued to generate great interest, owing to the well-reported adverse effects of overexposure to UV radiation [1-5]. Currently, several sunscreen formulations are on the market with active ingredients ranging from inorganic UV-filters such as titanium dioxide (TiO_2) and zinc oxide (ZnO) to organic UV-filters; examples of which include avobenzone, oxybenzone, homosalate, and octocrylene among many others [3,6]. Despite the many sunscreen formulations currently available, certain setbacks such as potential toxicity to humans and the environment as well as photo-instability have resulted in the banning of some UV-filters [7-10]. To this effect, sunscreen scientists have continued to search for safe and efficient UV-filters, seeking inspiration from natural sources including plants and microorganisms [11]. For example, in plants, sinapoyl malate (SM, see Figure 1A) found in the upper layer of Brassicaceous plants such as thale cress (*Arabidopsis thaliana*) has been reported to be the photoprotective agent [12,13]. In order to elucidate the photoprotection mechanism, the photodynamics of SM and its derivatives have also been studied [11,14-19]. Briefly, these studies have shown that following UV absorption, SM and its derivatives undergo an efficient and ultrafast energy relaxation mechanism predominantly *trans*-to-*cis* photoisomerization, which

accounts for their long-term photostability and photoprotective nature. Furthermore, an additional important advantage of these plant-based UV-filters is the broad UV-absorption profile that covers the UVB (280-315 nm) region of the solar spectrum and extending to the UVA (315-400 nm) where there is sparsity of efficient UV-filters.

In this work, we examine the potential photoprotection properties in a nature-inspired skincare active ingredient currently on the market. Detoxophane nc consisting of garden cress (*Lepidium sativum*) sprout extract (referred to as "cress sprout extract" henceforth), prepared in polar solubilizers and encapsulated with liposome (lipid vesicles), a versatile platform as a carrier for delivery of skincare products and drugs into the human body [20], has been developed by Mibelle Group Biochemistry for application as an anti-ageing skincare product [21]. This active ingredient helps to protect the skin cells against adverse environmental pollutants and other intrinsic reactive molecules (*e.g.* reactive oxygen species, ROS). However, since garden cress is closely related to thale cress, it is plausible to suggest that SM or other related derivatives could be responsible for the protection afforded by the plant. To this effect, we have focused our efforts on the photoprotection properties of both the cress sprout extract and Detoxophane nc through the use of transient electronic absorption spectroscopy (TEAS). This should enable us to access any potential effects of the complex surrounding environment on the photodynamics of both cress sprout extract and Detoxophane nc. The insight garnered may shed light on how the cress sprout extract can be potentially used as a UV-filter booster in skin-care formulations. Indeed, our results reveal that SM is the predominant UVB/UVA-filter in the cress sprout extract thereby offering photoprotection to the plant. The photodynamics of both cress sprout extract and Detoxophane nc are near-identical and compare well with the previously reported photodynamics of SM. Crucially, this suggests that the photoprotection properties of the SM in the cress sprout extract present in Detoxophane nc are not compromised by the surrounding environment.

2. Results

2.1. Steady-state spectroscopy

UV-Vis absorption spectra of the cress sprout extract and Detoxophane nc were measured in deionised water. As shown in Figure 1B, the UV absorption profile of the cress sprout extract displays a broad absorption band with an absorption maximum (λ_{max}) in the UV-A region (324 nm). The UV spectrum compares well with that of synthetic *trans*-SM in Figure 1B, having the same λ_{max} and similar absorption profile. This is an indication that the UV absorbing species in the cress sprout extract is either SM, a derivative, or a species with a similar absorption profile to SM. Furthermore, previous studies have reported that SM in nature occurs in the *trans*-isomer [17,22]. Hence, we might expect that SM in the cress sprout extract is in the same isomeric form. The agreement between the λ_{max} of synthetic *trans*-SM and cress sprout extract supports this expectation since the *cis*-isomer of SM has been reported to possess a broader and spectrally blue-shifted spectrum in a polar solvent [23]. The results of the ^{1}H NMR reported in the supporting information (SI) Figure S1 and S2 further suggest that the *trans*-isomer of SM is the absorbing species; indeed the coupling constant for H-3/H-4 are identical (16 Hz) and consistent with those expected for a *trans*-isomer rather than a *cis*-isomer.

In contrast to the cress sprout extract, the absorption of Detoxophane nc (Figure 1C) is rather broad and almost featureless; we suggest this is due to the dilution of the cress sprout extract in Detoxophane nc and the scatter from other components within the formulation. In this case, the UV absorbing species in the formulation would be hidden under the scattered spectrum from other components in the active ingredient.

Furthermore, the photostability of the cress sprout extract was explored in water as described in the methods section (see Section 4). The results presented in the SI Figure S3 revealed that the absorbing species demonstrates high photostability with only a 16 % reduction in the absorbance at the absorption maximum (λ_{max}) over 60 min of irradiation.

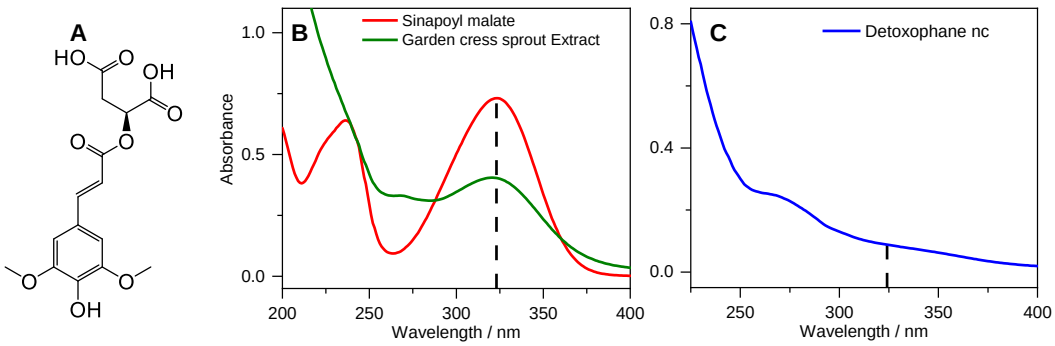

Figure 1. (A) Molecular structure of sinapoyl malate. UV-Vis spectra of samples obtained for (B) 0.01 mg/mL sinapoyl malate in water (red), and 0.1 mg/mL of garden cress sprout extract in water (green) and (C) Detoxophane nc diluted in ratio 1:100 in water.

2.2. Identification of the UV-absorbing species.

To identify the molecule responsible for the UV absorption in cress sprout, Ultra-High Performance Liquid Chromatography-High Resolution Mass Spectrometry (UHPLC-HRMS) measurements were carried out. The retention time on the UHPLC column as well as the high resolution mass spectra of the absorbing compound in the cress sprout were compared to those of synthetic *trans*-SM as reported in Figure 2. Figure 2A showed the UHPLC analysis of the garden cress sprout extract highlighting compounds eluting between 10-20 min and absorbing in the 210-390 nm range. The extracted ion chromatogram (EIC) for *m*/*z* values calculated for protonated SM (341.0867; $[C_{15}H_{16}O_9+H]^+$), for the ammonium SM adduct (358.1133; $[C_{15}H_{16}O_9+NH_4]^+$) and for the sodiated SM adduct (363.0687; $[C_{15}H_{16}O_9+Na]^+$) shown in Figure 2B revealed they were similarly retained on the UHPLC column with a retention time ~15.9 min (see also SI Figure S4 for the UV chromatogram of sample, standard as well as sample co-injected with the standard). The UV absorption spectrum of the cress sprout eluted at this time is shown in SI Figure S5 and matches that of the SM reported in Figure 1. The mass spectra at retention time 15.9 min., reported in Fig. 2C, also confirmed the presence of SM in the garden cress sprout extract. The same fingerprint was observed for the extract and for the synthetic SM standard and molecular formulae corresponding to the ions detected in the extract matched those of SM and SM adducts.

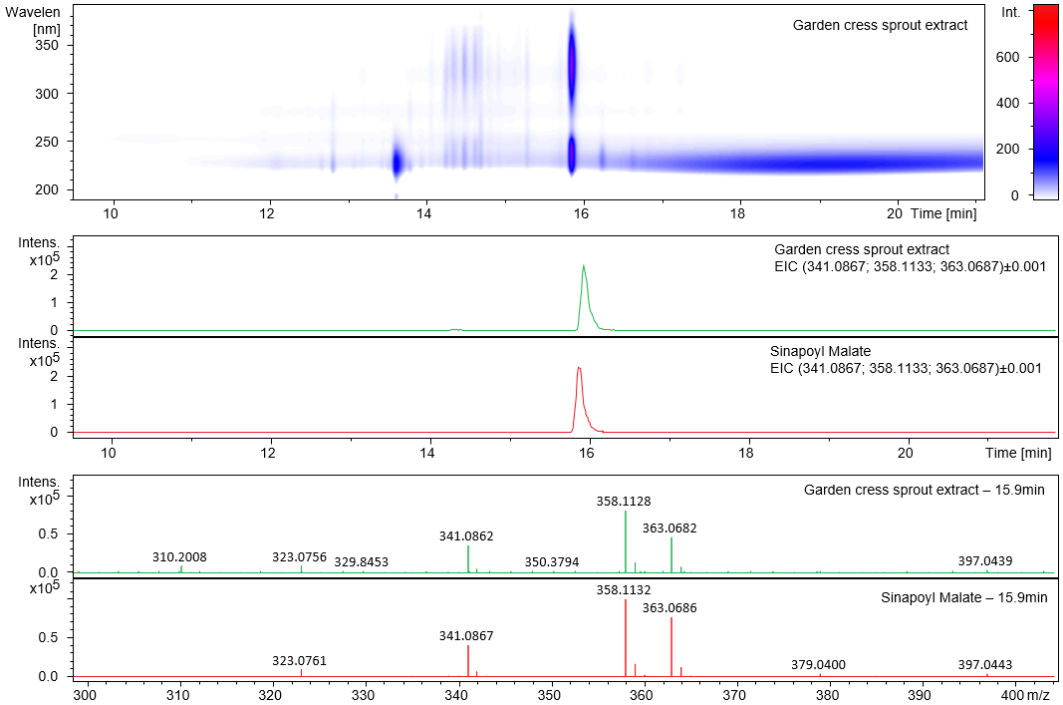

Figure 2. (A) UHPLC analysis of the garden cress sprout extract highlighting compounds eluting between 10-20 min and absorbing in the 210-390 nm range. (B) Extracted ion chromatogram of cress sprout (green) and sinapoyl malate standard (red) for *m*/*z* values calculated for $[SM+H]^+$, SM ammonium adduct and SM sodium adduct34. (C) Mass spectra for cress sprout, and sinapoyl malate at retention time 15.9 min.

2.3. Transient electronic absorption spectroscopy (TEAS)

We consider first the cress sprout extract. The transient electronic absorption (TEA) spectra measured following photoexcitation at 330 nm in a separate solution of dioxane and water are presented in Figure 3. We chose a weakly (dioxane) and strongly (water) interacting solvent, to investigate how the solvent-solute interaction influences the dynamics; this is also in keeping with previously reported studies for sinapate ester derivatives. Consequently, the assignment of the observed features based herein closely follows the literature [14,17,19,22,24-26]. For the cress sprout extract in dioxane (Figure 3A), the TEA spectra are dominated by three features. The first is a negative signal observed below ~350 nm (more visible in the line plots in Figure 3C) which is assigned to a ground state bleach (GSB) of the photoexcited SM molecules following comparison with the static UV-absorption spectrum. This feature persists throughout the maximum pump-probe delay time (Δt = 2 ns) of our experimental setup. The second is an intense positive signal peaking at ~400 nm, which predominantly decays to baseline within ~50 ps; a small component persists beyond 2 ns, and is discussed below. Finally, there is a second broad and weak absorption spanning the spectral region of ~500 – 700 nm. The two positive absorption features have been assigned previously in sinapate esters and similar systems to the excited state absorption (ESA) of the first singlet excited state (i.e. $S_n \leftarrow 1^1\pi\pi^*$) since initial photoexcitation promotes a $1^1\pi\pi^*$ state [14,17,19]. The TEA spectra of cress sprout extract in water shown in Figure 3B are also dominated by the three features seen in dioxane. In addition, a negative signal centred at ~470 nm is clearly present and assigned to stimulated emission (SE). This feature decays back to baseline by ~50 ps, a similar timescale on which the ESA at ~400 nm decays.

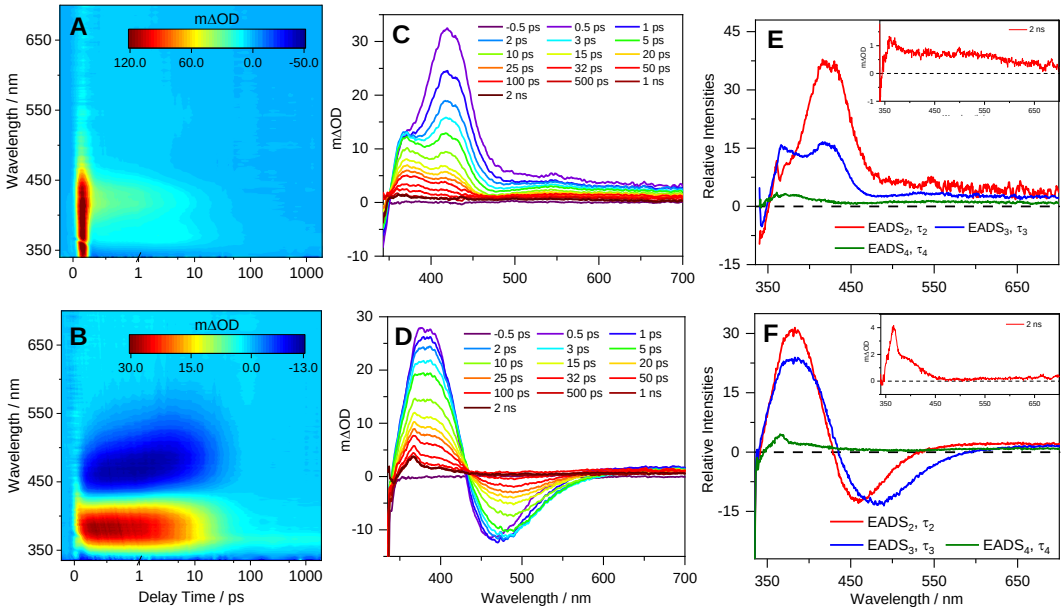

Figure 3. TEA spectra obtained for 0.1 g of cress sprout extract in 25 mL of (A) dioxane and (B) water, photoexcited at 330 nm and spectra are presented as false colour maps. The same data are presented as line plots of mΔOD vs probe wavelength at selected pump-probe delay times in (C) and (D) for cress sprout extract in dioxane and water, respectively. (E) and (F) show the evolution associated difference spectrum (EADS) for cress sprout extract in dioxane and water, respectively, produced by the fitting procedure. The inset in (E) and (F) show the transient absorption spectrum at the maximum available pump-probe delay of 2 ns.

Furthermore, the TEA spectra of the Detoxophane nc is shown in Figure 4. Briefly, the TEA spectra consist of three features, a GSB observed below ~350 nm, ESA centred at ~400 nm and a second broad ESA that spans ~500-700 nm. We add that the TEA spectra in Detoxophane nc more closely resemble the cress sprout extract in a weakly-interacting solvent (dioxane) as compared to a strongly interacting solvent (H_2O), evidenced by the absence of the SE feature. We return to discuss this in more detail below.

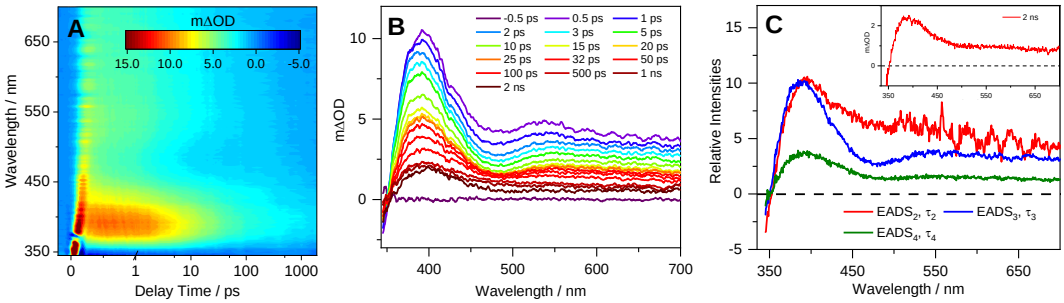

Figure 4. TEA spectra obtained for the bulk solution of Detoxophane nc photoexcited at 330 nm shown as a false colour map (A). The same data is presented as a line plot of mΔOD vs probe wavelength at selected pump-probe delay times in (B). The EADS is shown in (C) with the 2 ns transients presented as inset.

Quantitative insight into the photodynamical process observed in the TEA spectra of both cress sprout extract and Detoxophane nc is obtained by employing a global sequential ($A \xrightarrow{\tau_1} B \xrightarrow{\tau_2} C \xrightarrow{\tau_3} D\ldots$) decay model, implemented through the Glotaran software package [27,28]. The extracted time constants are reported in Table 1 while the quoted errors are those returned by the fitting software to 2σ, though the quality of the fits are better evaluated by inspecting the associated residuals reported in the SI Figure S6. Where the error returned by the fitting package was shorter than the instrument response time, the error is quoted as half the instrument response, as determined via the solvent-only transients presented in the SI Figure S7.

Table 1. Time constants and associated errors extracted from fitting the TEA spectra collected for cress sprout extract in water and dioxane, and Detoxophane nc.

Sample	τ_1 / fs	τ_2 / ps	τ_3 / ps	τ_4 / ns
Cress sprout extract (water)	120 ± 50	1.04 ± 0.05	17.13 ± 0.17	> 2
Cress sprout extract (dioxane)	60 ± 40	0.91 ± 0.04	14.84 ± 0.35	> 2
Detoxophane nc	60 ± 40	0.52 ± 0.04	11.90 ± 0.20	> 2

3. Discussion

We now discuss the implications of our results with respect to photoprotection, drawing on different aspects of the experimental studies. The UV-vis and UHPLC-HRMS spectra suggest that the absorbing species in the cress sprout extract is SM. In Detoxophane nc bulk solution, the UV-absorption is featureless due to the lower concentration of the absorbing species and scattering effect of other components of the formulation.

With regards to the ultrafast photodynamics of the cress sprout extract and the Detoxophane nc solution, we draw on our experimental results and previous studies, on SM and its derivatives [14,17,19,22,24-26], to assign the dynamical processes to the extracted time constants reported in Table 1 and discuss the implications of our findings. This decision is supported by the similarity between the TEA spectra obtained in the current work and those reported previously for SM and its derivatives, as well as the molecular identity confirmation from mass spectrometry. Focussing initially on τ_1, previous studies have shown that following initial photoexcitation to the $1^1\pi\pi^*$ state, SM and its derivatives tend to undergo rapid geometry and vibrational relaxation out of the Franck-Condon region, along with any solvent rearrangement [14,17,22]. However, we note that τ_1 obtained for cress sprout extract in dioxane and Detoxophane nc are within our instrument response (~80 fs). We, therefore, attribute τ_1 to the aforementioned dynamical processes together with coherent artefacts of the instrument response function.

The dynamical process associated with τ_2 has been assigned to a number of different processes previously, one of such process is the internal conversion (IC) of the $1^1\pi\pi^*$ state to the $2^1\pi\pi^*$ state via $1^1\pi\pi^*/2^1\pi\pi^*$ conical intersection (CI) [14]. However, computational studies in implicit solvent have found that only $1^1\pi\pi^*$ is involved in the relaxation mechanism of SM [22,29]. As such subsequent studies assigned this process to vibrational cooling of the $1^1\pi\pi^*$ state [19]. This seems plausible given the blue shifting of $EADS_3$ compared to $EADS_2$ (Figure 3E, F and 4C). The dynamical process associated with τ_3 is then assigned to population flowing from the $1^1\pi\pi^*$ state to the ground state, along the *trans-cis* photoisomerisation coordinate, mediated by a $1^1\pi\pi^*/S_0$ CI. This dynamical process results in a fraction of the excited state population reforming the original *trans*-isomer while another fraction completes the isomerisation along the allylic C=C double bond to generate the *cis*-isomer photoproduct. The *cis*-isomer photoproduct accounts for the absorption of $EADS_4$ (at ~360 nm) with a time constant τ_4 which is > 2 ns [14,15,17,19,22,25,26,30].

The assignment of $EADS_4$ to the *cis*-isomer is supported through comparison of the transient absorption profile obtained at Δt = 2 ns shown as an inset in Figure 3E,F and 4C to those reported for SM and its derivatives previously [14,30], which show an identical long-lived feature and assigned to *cis*-isomer.

While the overall photodynamics of the SM within cress sprout extract and Detoxophane nc are largely complete within 100 ps, differences in the time constants and spectral profiles are observed and warrant discussion. We briefly focus our discussion on the difference between SM in Detoxophane nc compared to SM in cress sprout extract in both dioxane and water. With regards to the time constants, those extracted from Detoxophane nc are predominantly shorter than the corresponding time constants extracted from the cress sprout extract in both dioxane and (most notably) water. The longer time constants in water are in line with previous studies of SM and its derivatives in polar solvents, compared nonpolar counterpart [14,29]. This difference in time constants in different polarity solvents is likely due to changes in the potential energy surface of SM in the excited state;

this results in a higher energy barrier to overcome along the relaxation coordinate in polar solvents. In terms of spectral profiles, in previous studies of SM and its derivatives [14,17,19,22,25,26], SE is a characteristic feature seen in the TEA spectra in polar solvents. The absence of SE in the TEA spectra of Detoxophane nc suggests that (i) the majority of the cress sprout extract is encapsulated within the lipid vesicles; and (ii) the host (encapsulation) and guest (SM in the cress sprout extract) interaction within the cage is more complex than a simple interface of SM, polar solubilizer and hydrophilic end of the lipid vesicles. Importantly, this complex interaction between the host and guest only mildly perturbs the photodynamics of the absorbing species, as is the case in weakly perturbing, non-polar solvents.

Taken together, the ultrafast photodynamics of SM in Detoxophane nc are not compromised by other components within the formulation. This is an important requirement of a UV-filter for sunscreen formulation, enabling the UV-filter to dissipate the excess energy absorbed safely and bypassing potentially harmful side reactions such as the generation of reactive oxygen species. Likewise, the ultrafast relaxation processes ensure the UV-filter is effectively recycled, (*i.e*. retains its molecular integrity), to maintain photoprotection.

4. Materials and Methods

4.1. Steady-state spectroscopy

All solvents used were analytical grade unless otherwise stated.

The cress sprout extract and Detoxophane nc were studied with spectroscopy as received from "Mibelle Group Biochemistry" without further purification. For the steady-state measurement, 0.1 mg/mL of the cress sprout extract was dissolved in deionised water. The UV-vis measurements were taken in a 1 cm path length quartz cuvette using Cary 60 spectrometer (Agilent Technologies). The same measurement was repeated for Detoxophane nc diluted in deionised water (1:100). SM was synthesised as described in previous studies [31,32].

^{1}H NMR spectra data were collected in deuterium oxide (Sigma Aldrich) using Bruker Avance III HD, 400 MHz.

4.2. Identification of the UV-absorbing species

The cress sprout extract was prepared for measurement with UHPLC-HRMS for identification of the UV-absorbing species as follows. The cress sprout extract was sequentially extracted in 50% HPLC-grade methanol at 4^{o}C overnight followed by sonication the next day. After extraction, the solvent was pooled together, centrifuged at 4000 rpm for 30 minutes to get rid of debris and the clear solvent was evaporated using the centrifugal evaporator (SP Genevac EZ-2 Series). The crude extract was then resuspended in 50:50 v/v water: methanol, filtered using an amicon ultra 3K cut-off filter for UHPLC-HRMS analysis. In like manner, synthesised *trans*-SM was prepared to a concentration of 20 μM in 50:50 v/v water: methanol as standard for UHPLC-HRMS analysis. Analysis was carried out with 2 μL sample injection through a reverse-phase column (Zorbax Eclipse plus C18, size 2.1 x 100 mm, particle size 1.8 μm) connected to a Dionex 3000 RS UHPLC hyphenated to Bruker Ultra High-Resolution Q – TOP MS Maxis II mass spectrometer using electrospray ionization (ESI) positive mode. A m/z range of 50-3000 was used. A gradient elution method was programmed by increasing solvent B from 0-100% for 30 mins; (solvent A = 0.1 % (v/v) formic acid in water and solvent B = acetonitrile with 0.1 % formic acid). The system was then equilibrated for 15 min before the next injection.

4.3. Transient electronic absorption spectroscopy (TEAS)

The femtosecond (fs) TEAS setup and procedure used to explore the photodynamics of the cress sprout extract and Detoxophane nc has been detailed previously [16,18,33-35], and only information specific to the present experiment is reported here. For the cress

sprout extract, 0.1 g of the dried extract was dissolved in 25 mL of deionised water and separately in dioxane whereas the Detoxophane nc was used for TEAS as received without further dilution. In all cases, the pump excitation wavelength was set at 330 nm. The sample was delivered through a demountable Harrick Scientific flow-through cell equipped with two CaF_2 windows separated by 100 (950) μm polytetrafluoroethylene spacers for cress sprout extract (Detoxophane nc), thereby defining the optical path length of the sample. The samples were circulated using a diaphragm pump (SIMDOS, KNF) recirculating from a 25 mL sample reservoir to ensure each pump-probe pulse interacts with a fresh sample, with a maximum pump-probe delay of 2 ns.

5. Conclusions

In conclusion, all our studies revealed that the UV-absorbing species in cress sprouts extract is mainly sinapoyl malate. Furthermore, we have found through transient electronic absorption spectroscopy that the photoprotection properties of the cress sprout extract mirrors that of sinapoyl malate. Finally, our studies revealed that the photoprotection properties of the sinapoyl malate in the cress sprout extract present in Detoxophane nc is not compromised by the formulation environment. While Detoxophane nc is not recommended as a substitute for organic or inorganic registered UV-filters for sunscreen applications, the current study suggests that it may offer additional photoprotection to end-user as a UV-filter booster.

Supplementary Materials: The following are available online at www.mdpi.com/xxx/s1, Figure S1: Residuals for the Sequential Fit to the TEA Spectra, Figure S2: Instrument Response Function.

Author Contributions: Conceptualization, V.G.S. and S.P.; investigation, T.T.A. and N.A.; data analysis, T.T.A., J.M.W, N.A., and C.C.; writing-original draft preparation, T.T.A.; writing—review and editing, T.T.A., J.M.W, N.A., C.C., S.P. and V.G.S.; supervision, C.C. and V.G.S; project administration, S.P. All authors have read and agreed to the published version of the manuscript.

Funding: This research was funded by The University of Warwick Chancellor Scholarship for International Students.

Data Availability Statement: The datasets presented in this study can be found in online repositories. The names of the repository/repositories is Zenodo repository.

Acknowledgments: The authors would like to thank Mibelle Group Biochemistry for supplying the samples of garden cress sprout extract and Detoxophane nc. The authors thanks Professor Florent Allais and his team for supplying the sinapoyl malate standard used. T.T.A. and N.A. thanks The University of Warwick for Ph.D. studentship through the Chancellor Scholarship. J.M.W. acknowledges the support of FetOpen grant BoostCrop (Grant Agreement 828753). V.G.S. thanks the Royal Society and Leverhulme Trust for a Royal Society Leverhulme Trust Senior Research Fellowship, the Royal Society for a Royal Society Industry Fellowship, and the EPSRC (UK) under Grant No. EP/N010825/1.

Conflicts of Interest: The authors declare no conflict of interest.

Sample Availability: Samples of the cress sprout extract and Detoxophane nc are available from the authors.

References

1. Dahle, J. and E. Kvam, *Induction of delayed mutations and chromosomal instability in fibroblasts after UVA-, UVB-, and X-radiation.* Cancer Res., 2003. **63**(7): p. 1464-1469.
2. Baker, L.A., et al., *Photoprotection: extending lessons learned from studying natural sunscreens to the design of artificial sunscreen constituents.* Chem. Soc. Rev., 2017. **46**(12): p. 3770-3791.
3. Rodrigues, N.D.N., M. Staniforth, and V.G. Stavros, *Photophysics of sunscreen molecules in the gas phase: a stepwise approach towards understanding and developing next-generation sunscreens.* Proc. R. Soc. A, 2016. **472**(2195): p. 20160677.
4. Rai, R. and C. Srinivas, *Photoprotection.* Indian J. Dermatol. Ve., 2007. **73**(2): p. 73.
5. Gallagher, R.P. and T.K. Lee, *Adverse effects of ultraviolet radiation: a brief review.* Progress in biophysics and molecular biology, 2006. **92**(1): p. 119-131.

6. Gasparro, F.P., *Epilogue: new perspectives in sunscreen photobiology*, in *Sunscreen Photobiology: Molecular, Cellular and Physiological Aspects*. 1997, Springer. p. 177-186.
7. Boehm, F., et al., *Lichens–Photophysical studies of potential new sunscreens.* Journal of Photochemistry and Photobiology B: Biology, 2009. **95**(1): p. 40-45.
8. Downs, C., et al., *Toxicological effects of the sunscreen UV filter, benzophenone-2, on planulae and in vitro cells of the coral, Stylophora pistillata.* Ecotoxicology, 2014. **23**(2): p. 175-191.
9. Downs, C.A., et al., *Toxicopathological effects of the sunscreen UV filter, oxybenzone (benzophenone-3), on coral planulae and cultured primary cells and its environmental contamination in Hawaii and the US Virgin Islands.* Archives of environmental contamination and toxicology, 2016. **70**(2): p. 265-288.
10. Schaap, I. and D.M. Slijkerman, *An environmental risk assessment of three organic UV-filters at Lac Bay, Bonaire, Southern Caribbean.* Marine pollution bulletin, 2018. **135**: p. 490-495.
11. Abiola, T.T., A.L. Whittock, and V.G. Stavros, *Unravelling the Photoprotective Mechanisms of Nature-Inspired Ultraviolet Filters Using Ultrafast Spectroscopy.* Molecules, 2020. **25**(17): p. 3945.
12. Milkowski, C. and D. Strack, *Sinapate esters in brassicaceous plants: biochemistry, molecular biology, evolution and metabolic engineering.* Planta, 2010. **232**(1): p. 19-35.
13. Nguyen, V., et al., *Sinapic Acid and Sinapate Esters in Brassica: Innate Accumulation, Biosynthesis, Accessibility via Chemical Synthesis or Recovery From Biomass, and Biological Activities.* Front. Chem., 2021. **9**: p. 350.
14. Baker, L.A., et al., *Ultrafast photoprotecting sunscreens in natural plants.* J. Phys. Chem. Lett., 2015. **7**(1): p. 56-61.
15. Baker, L.A., et al., *Gas‐Solution Phase Transient Absorption Study of the Plant Sunscreen Derivative Methyl Sinapate.* ChemPhotoChem, 2018. **2**(8): p. 743-748.
16. Abiola, T.T., et al., *New Generation UV-A Filters: Understanding their Photodynamics on a Human Skin Mimic.* J. Phys. Chem. Lett., 2021. **12**: p. 337-344.
17. Horbury, M.D., et al., *Investigating isomer specific photoprotection in a model plant sunscreen.* Chem. Commun., 2018. **54**(8): p. 936-939.
18. Horbury, M.D., et al., *Towards symmetry driven and nature inspired UV filter design.* Nat. Commun., 2019. **10**(1): p. 1-8.
19. Horbury, M.D., et al., *Elucidating nuclear motions in a plant sunscreen during photoisomerization through solvent viscosity effects.* Phys. Chem. Chem. Phys., 2017. **19**(31): p. 21127-21131.
20. Has, C. and P. Sunthar, *A comprehensive review on recent preparation techniques of liposomes.* J. Liposome Res., 2020. **30**(4): p. 336-365.
21. *Mibelle Group Biochemistry: Detoxophane nc*. [cited 2021 August]; Available from: https://mibellebiochemistry.com/detoxophane.
22. Luo, J., et al., *Ultrafast barrierless photoisomerization and strong ultraviolet absorption of photoproducts in plant sunscreens.* J. Phys. Chem. Lett., 2017. **8**(5): p. 1025-1030.
23. Hanson, K.M., et al., *Effects of solvent and micellar encapsulation on the photostability of avobenzone.* Photochem. Photobiol. Sci., 2020. **19**(3): p. 390-398.
24. Horbury, M.D., et al., *Exploring the photochemistry of an ethyl sinapate dimer: an attempt toward a better ultraviolet filter.* Frontiers in chemistry, 2020. **8**: p. 633.
25. Zhao, X., et al., *Substitution Dependent Ultrafast Ultraviolet Energy Dissipation Mechanisms of Plant Sunscreens.* J. Phys. Chem. Lett., 2019. **10**: p. 5244-5249.
26. Zhao, X., et al., *New Insight into the Photoprotection Mechanism of Plant Sunscreens: Adiabatic Relaxation Competing with Nonadiabatic Relaxation in the cis→ trans Photoisomerization of Methyl Sinapate.* J. Phys. Chem. Lett., 2019. **10**(15): p. 4197-4202.
27. Snellenburg, J., et al., *Glotaran: A Java-based graphical user interface for the R package TIMP.* J. Stat. Softw., 2012: p. 49.
28. Mullen, K.M. and I.H.M. Van Stokkum, *TIMP: an R package for modeling multi-way spectroscopic measurements.* J. Stat. Softw., 2007. **18**(3): p. 1-46.
29. Zhao, X., et al., *Theoretical and spectroscopic investigation on ultrafast nonadiabatic photoprotective mechanism of novel ultraviolet protective compounds inspired by natural sunscreens.* J. Lumin., 2020. **223**: p. 117228.
30. Baker, L.A., et al., *Conservation of ultrafast photoprotective mechanisms with increasing molecular complexity in sinapoyl malate derivatives.* ChemPhysChem, 2020. **21**(17): p. 2006.
31. Allais, F., S. Martinet, and P.-H. Ducrot, *Straightforward total synthesis of 2-O-feruloyl-L-malate, 2-O-sinapoyl-L-malate and 2-O-5-hydroxyferuloyl-L-malate.* Synthesis, 2009. **2009**(21): p. 3571-3578.
32. Peyrot, C., et al., *Expeditious and sustainable two-step synthesis of sinapoyl-l-malate and analogues: towards non-endocrine disruptive bio-based and water-soluble bioactive compounds.* Green Chem., 2020. **22**(19): p. 6510-6518.
33. Horbury, M.D., et al., *Photoisomerization of ethyl ferulate: A solution phase transient absorption study.* Chem. Phys. Lett., 2017. **673**: p. 62-67.
34. Greenough, S.E., et al., *Solvent induced conformer specific photochemistry of guaiacol.* Phys. Chem. Chem. Phys., 2014. **16**(30): p. 16187-16195.
35. Greenough, S.E., et al., *Ultrafast photo-induced ligand solvolysis of cis-[Ru (bipyridine) 2 (nicotinamide) 2] 2+: experimental and theoretical insight into its photoactivation mechanism.* Phys. Chem. Chem. Phys., 2014. **16**(36): p. 19141-19155.